Particle Distribution in Unbaffled Stirred Vessels

Alessandro Tamburini*, Francesca Scargiali, Giorgio Micale, Alberto Brucato

Dipartimento dell'Innovazione Industriale e Digitale - Ingegneria chimica, gestionale, informatica, meccanica, Università di Palermo, Viale delle Scienze Ed. 6, 90128 Palermo (ITALY)
alessandro.tamburini@unipa.it

The present work is devoted to providing an insight into the solid-particle distribution within top-covered unbaffled stirred tanks via purposely collected local experimental data. Experiments were carried out on a lab-scale unbaffled stirred tank by making use of a recently introduced technique named Laser Sheet Image Analysis (LSIA). In its original formulation, the technique includes an image post-processing procedure to delete reflection effects on results. In the framework of the present work, a method combining the use of purposely produced fluorescent particles and a suitable camera high pass filter was devised and presented. Results collected with (new method) and without (old fashion) fluorescent particles were compared for comparison purposes and a satisfactory agreement was found, thus validating both the procedures devised to delete reflections.

LSIA technique in the novel version was used to investigate the distribution of solid particles at different agitation speeds in an unbaffled tank stirred by either a marine propeller or by a Rushton turbine. On overall, collected results show that the propeller configuration provides somewhat better particle distribution throughout the tank as compared with Rushton turbine operated at the same agitation speed. The two stable toroidal attractors for solid particles there observed are recognizable also here, though with a configuration significantly different due to the diverse flow fields.

1. Introduction

Mixing of solid particles into liquids via mechanical agitation is frequently encountered in a number of industrial processes (Oldshue, 1983). Both particle suspension (Tamburini et al., 2011a) and distribution (Tamburini et al., 2013a) are topics of crucial importance in the process industry. Such operations are usually performed within cylindrical tanks provided with "baffles" (metal strips vertically deployed along vessel walls), although there are many cases in which these may be undesirable (e.g. due to ease of cleaning, risk of giving rise to dead zones with viscous liquids, etc.) (Assirelli et al., 2007; Hekmat et al, 2008; Tamburini et al., 2011b). In recent years, a growing awareness of the potential advantages of unbaffled vessels with respect to baffled ones has become widespread (Brucato et al., 2010; Tamburini et al., 2012; Busciglio et al., 2014; Scargiali et al., 2014) especially in bio-related processes (Scargiali et al., 2013; Montante et al., 2014; Tamburini et al., 2016). Among these advantages, the lower power drawn (in unbaffled tanks compared to corresponding baffled tanks) for achieving complete suspension conditions is certainly the most worthy (Tamburini et al., 2014; Wang et al., 2014). However, there still is a poor knowledge of these reactors, especially for multiphase systems, that inhibits exploiting their full potential (Sardeshpande et al., 2016; Busciglio et al., 2016). In this regard, aim of the present work is providing 2-D concentration maps of solid particles in a top-covered unbaffled stirred tank by making use of a recently developed optical non-intrusive technique named *Laser Sheet Image Analysis* (Tamburini et al., 2013b).

2. Experimental set-up

The experimental system employed is constituted by the investigated stirred tank provided with an air-removal system and the LSIA apparatus.

The investigated vessel was a flat-bottomed, top-covered, unbaffled, cylindrical tank with an inner diameter of T=0.19m and height H=T, as shown in a previously published paper (Tamburini et al., 2013b). Either a

standard six bladed Rushton turbine with a diameter D=T/2 placed at a clearance C=T/3 or a marine propeller with a diameter D=T/2.4 placed at a clearance C=T/4 was employed for the experiments. In order to avoid optical distortion problems, the stirred vessel was placed into a bigger rectangular tank, whose walls were perpendicular to the laser and the videocamera directions.

The LSIA apparatus consists of the illumination system (pulsed laser), the acquisition system (Dantec PIV), the synchronization system (Dantec processor, Flow Map 1500) and the PC with the relevant software (Dantec Flow Manager). Full details can be found in the previous work by Tamburini et al. (2013b).

The time between two subsequent recordings (111 μs) was never a multiple of the impeller rotation frequency, in order to get angle-averaged rather than angle resolved measurements.

The tank was filled with deionised water and solid particles with a concentration of 0.2 g/L, hereafter indicated as C_m. In-house purposely made fluorescent particles (ρ = 1400 kg/m^3) (see the following paragraph) whose diameter was 425-500μm were employed in the vessel stirred at different angular velocities. Table 1 reports a summary of the experiments performed.

Table 1: Experiments performed summary data.

Top-covered unbaffled vessel stirred by a standard Rushton turbine					
Fluorescent and non-fluorescent Particles					
Diameter 425-500 µm	------	300 RPM	400 RPM	500 RPM	600 RPM
Top-covered unbaffled vessel stirred by a marine propeller					
Fluorescent Particles					
Diameter 425-500 µm	200 RPM	300 RPM	400 RPM	500 RPM	600 RPM

3. LSIA fundamentals

LSIA technique is based on a suitable probabilistic post-processing of the videocamera acquired snapshots within a Matlab routine. The particles are stochastically hit by the laser sheet, thus appearing as bright little points (Figure 1). Their instantaneous position within the laser sheet plane is captured by the camera which is synchronized with the laser. Each grey scale image acquired is converted into a 2-D matrix whose each element corresponds to a single pixel of the Charge-Coupled Device (CCD). The matrix is binarized by choosing a suitable threshold grey-level so that each 1 of the matrix corresponds to a bright object. In LSIA original formulation, all matrixes are filtered in order to identify the particles and delete possible reflections and spurious white peaks (both visible in Figure 1A for glass particles). After these removal procedure, each 1 of the final matrixes represents a particle centre. By acquiring a statistically sufficient number of images (about 2000) and summing their relevant position matrixes it is possible to obtain a particle presence probability distribution map over the laser sheet. This can be in its turn converted into the local mass concentration C through a constant factor related to the particle mass loaded in the tank. Full details on the technique are reported in in the previous work by Tamburini et al. (2013b). As reported above, in this original formulation, the technique includes an image post-processing procedure to delete reflection effects on results. Here, a new methodology is proposed to solve the light reflection issue.

3.1 Light reflection removing procedure

Light reflections can be confused with particles during image processing, so leading to unreliable particle concentration assessments. The adoption of particles labelled with the Rhodamine B is here investigated as an alternative to solve the reflection issue. These particles were prepared by mixing a thermosetting resin with its relevant catalyst (weight ratio 2:1), a glass charge necessary to increase the final particle density and the Rhodamine B. The obtained polymer pieces were ground and sieved. The density of the obtained particles was experimentally found equal to about 1400 kg/m^3. During the experiments performed with fluorescent particles, a high-pass filter with a threshold wave length value of 570nm was employed. The Rhodamine B hit by the laser sheet emits the light at a wave length of about 590nm (Figure 2A). Therefore, thanks to the adoption of the high-pass filter, only the illuminated fluorescent particles are visible, as shown in Figure 1B, (while all reflections with a wavelength of 543nm are filtered, Figure 2A). Note that, some reflections would however be present if blackening of metallic surfaces with paint is not performed. For example, Unadkat et al. (2009) find unexpected high values of solid concentrations in the proximity of the impeller: the light reflected by particles can hit the metal-made shaft and the impeller, thus resulting in a secondary reflection which can pass over the filter and provide the unphysical highlighted areas near the stirrer.
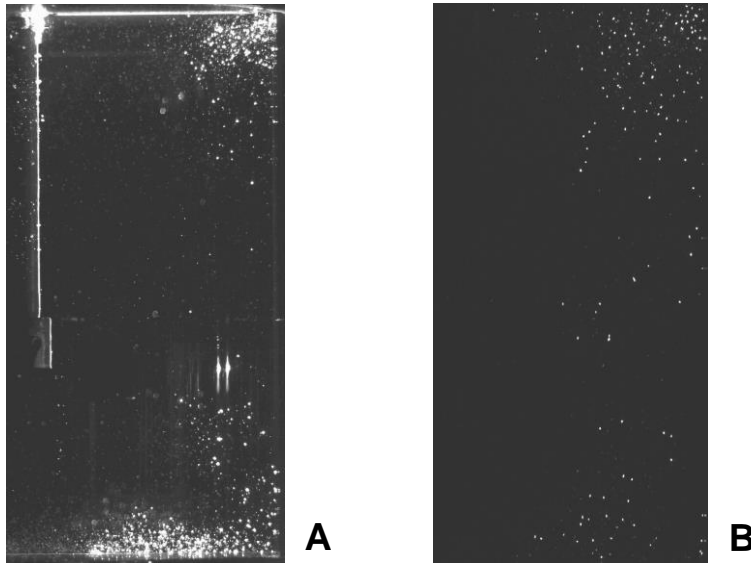
Figure 1: An example of system snapshot for: (A) 425-500 μm glass particles; (B) 425-500 μm fluorescent particles.

4. Results and discussion

4.1 Standard Rushton Turbine

In order to verify the effectiveness of the novel light reflections removal procedure, two identical set of particles were prepared with the procedure previously described in section 3: one set with added Rhodamine B, the other without Rhodamine B. Relevant results were compared to each other. The worst example of the radially averaged axial profiles of solid concentration (i.e. C_{rm}) resulting from these experiments is shown in Figure 2B: the two profiles are quite similar thus indicating that the two light reflections removal procedure are able to provide reliable results, although with some differences in the regions where the highest concentrations of particles are found. This occurrence is not surprising since these regions generate the highest number of peaks and reflections, but give rise to discrepancies which may be quantified up to an engineering acceptable 8 %. Note that the concentration maps obtained for the case of this radial impeller (not reported for brevity) show the presence of two stable toroidal attractors for solid particles as already described in previous works (Tamburini et al., 2009; 2013b).
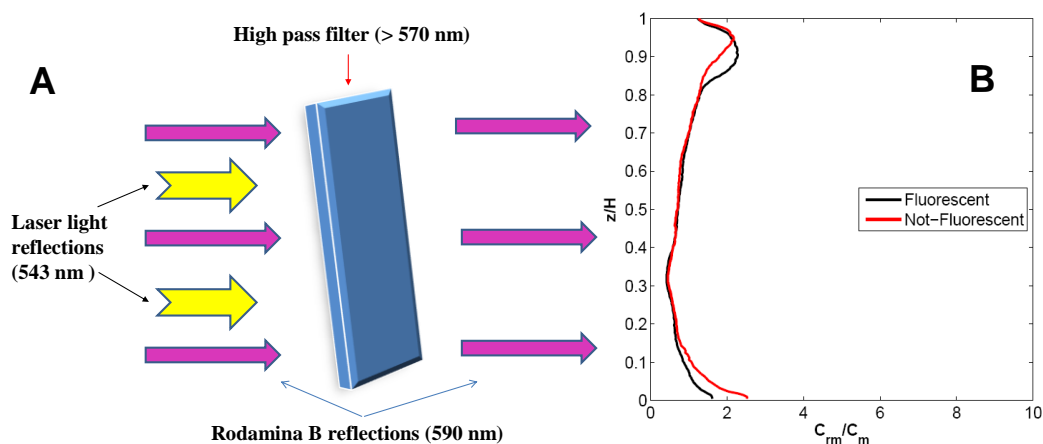

Figure 2: (A) Principle of the novel reflection removal procedure. (B) Radially averaged axial profile of solid concentration C_{rm} normalized with C_m for the case of particles in-house made with and without Rhodamine B at 400 RPM.

4.2 Propeller

Experiments were run also for the case of an unbaffled tank stirred by a marine propeller.

The same fluorescent particles of 425-500 μm with density of about 1400 kg/m^3 previously used were selected for these experiments. Five different impeller velocities were investigated; relevant results are shown in Figure 3. Note that, the just suspension speed N_{js}, was visually estimated as being smaller than 200 RPM (which coincides with the minimum impeller speed here investigated). At all rotational speeds, the particle distribution within the vessel is markedly different with respect to the case of the previously investigated Rushton turbine (not shown here for the sake of concision, yet visible in Tamburini et al, 2013b). Particles are dispersed as a result of the main convective flows generated by the propeller. These involve a discharge stream from the propeller at about 45° with respect to the shaft axis, that reaches the bottom and is deviated outwards, up to reaching vessel wall and being deflected vertically, so giving rise the main circulation loop in the vessel, characterized by weaker and weaker velocities while moving upwards. In the volume left out from the main loop, centrally located between the bottom and the propeller discharge stream, a smaller, counter-rotating circulation loop is formed. The presence of these two loops generates different equilibrium conditions at different angular velocities:

- at impeller speeds between 200 RPM and 400 RPM most particles are found in the lower part of the vessel, and especially in the inner counter-rotating loop. Particles in contact with tank bottom do not form a stable sediment, but they rather roll over the bottom while azimuthally circulating.

- when agitation speed is progressively increased, particles tend to progressively fill the main circulation loop, so distributing in the upper region of the vessel, with a tendency to accumulate in the proximity of the lateral tank wall, as it is evident at 600 RPM. Even at these relatively large velocities the presence of particles rolling on the bottom can be still observed, though reduced in quantity. At these relatively high velocities, the secondary ring effect increases because of higher mean fluid velocities that allow suspended particles to reach higher heights before moving downward towards the propeller. It is worth noting that the two stable attractors for suspended particles observed in the case of Rushton turbines are also found here, though their shapes are markedly different due to the different flow patterns generated by propeller action.
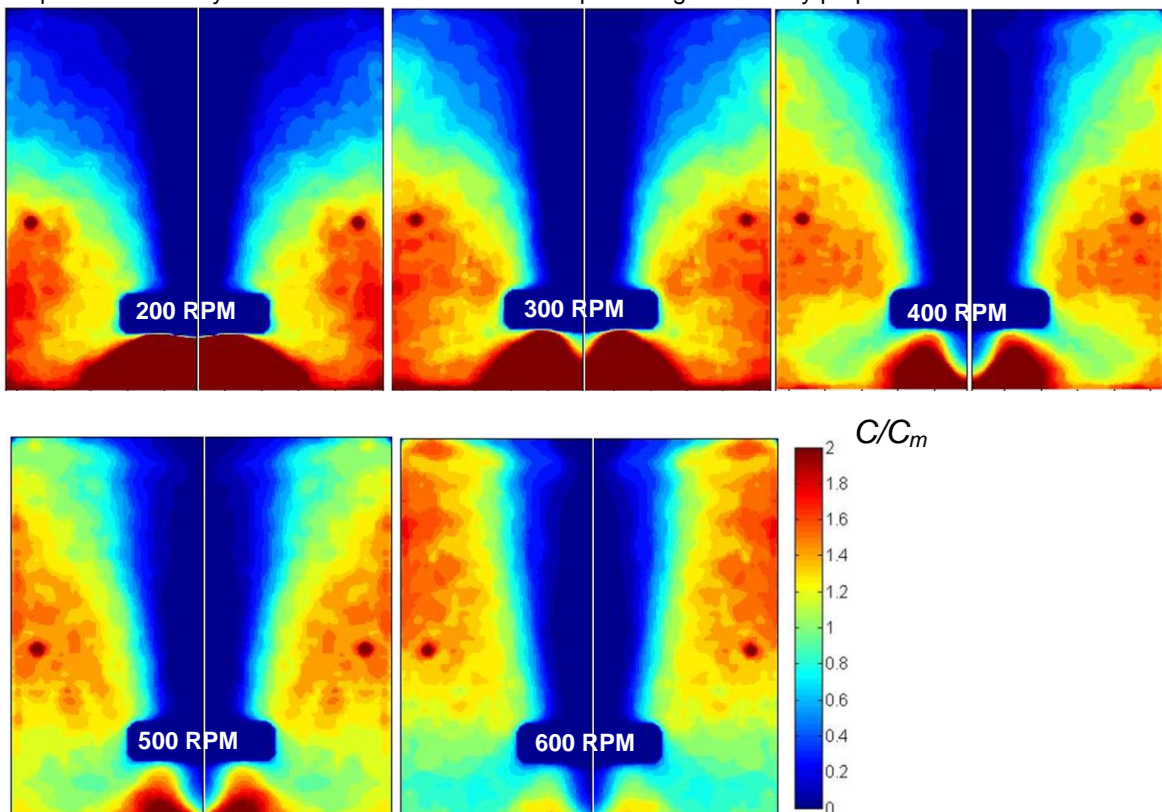

Figure 3: Contour plots of normalized local solid concentration (on the laser sheet plane) for 425-500 μm fluorescent particles at different propeller rotational velocities.
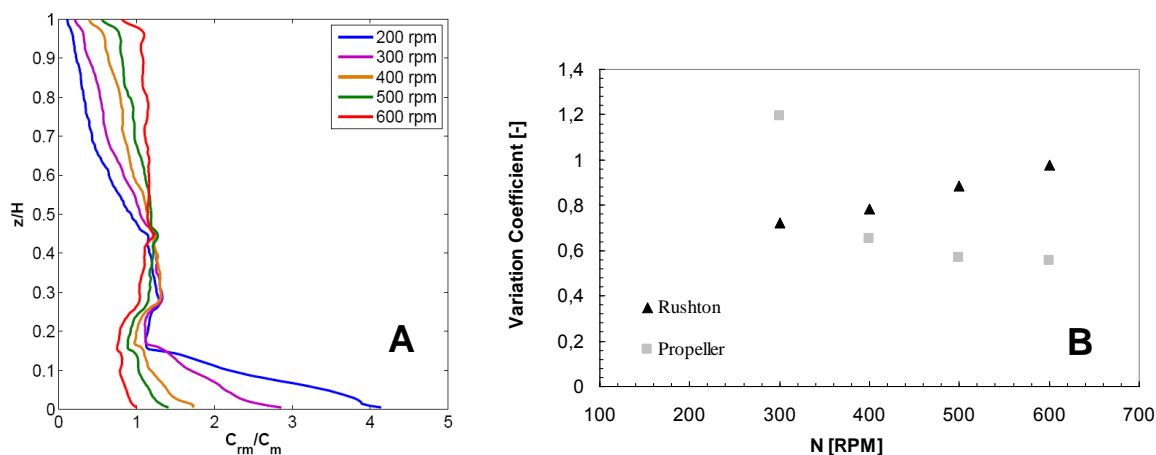
Figure 4: (A) Radially averaged axial profiles of normalized solid concentration for 425-500 μm fluorescent particles at different propeller rotational velocities. (B) Comparison of normalized standard deviations for the two types of turbine (425-500 μm fluorescent particles).

The radially averaged axial profiles of normalized solid concentration shown in Figure 4A indicate that no clear liquid layer exists in the upper part of the vessel at all the investigated impeller speeds. These profiles also confirm that an increase in impeller speed leads to a higher degree of homogeneity as a result of the decrease of solid concentration in the lower part of the vessel and a consequent increase in the upper part of the vessel. By comparing these results with those obtained in the case of the radial impeller it is clear that the two impellers provide a very different effect on solid particle distribution. As the rotational speed increases, the propeller generates a better dispersion of solid particles, while Rushton turbine leads to concentrate them towards the two tori, as it can be appreciated in Figure 4B where the variation coefficients (i.e. standard deviations normalized by their mean) obtained with the two impellers are compared at different rotational speeds for the same particles. This evidence suggests the adoption of one impeller or the other depending on process requirements.

5. Conclusions

Results collected with fluorescent particles (new method) and with hydraulically identical normal particles (old method) were compared with each other and a satisfactory agreement was found, thus validating for both data sets the procedures devised to delete reflections. It may be inferred that the LSIA technique can be reliably applied to solid-liquid dispersions and can provide experimental data suitable for computational models validation.

On overall, collected results show that the propeller-configuration provides a better *particle distribution* throughout the tank, especially as the propeller speed is increased, while a stronger *concentration effect* was observed for the Rushton-configuration, due to the relevant stronger action of the previously described toroidal attractors for solid particles. This suggests that in unbaffled tanks, quite different process aims might be pursued by adopting different geometrical configurations.

Future improvements of the LSIA technique will concern (i) its application to dense suspensions via a suitable Refractive Index Matching of the two phases as suggested by Micheletti and Yianneskis (2004), and (ii) its coupling with a PIV analysis (simply by using another acquisition camera, Unadkat, 2009) to obtain simultaneously information on the fluid and particle flow fields inside the vessel.

Reference

Assirelli M., Bujalski W., Eaglesham A., Nienow A.W., 2008, Macro- and micromixing studies in an unbaffled vessel agitated by a Rushton turbine. Chem. Eng. Sci., 63, 35-46.

Brucato A., Cipollina A., Micale G., Scargiali F., Tamburini A., 2010, Particle suspension in top-covered unbaffled tanks. Chem. Eng. Sci., 65 (10), 3001-3008.

Busciglio A., Grisafi F., Scargiali F., Brucato A., 2014, Mixing dynamics in uncovered unbaffled stirred tanks, Chemical Engineering Journal, 254, 210-219.

Busciglio A., Scargiali F., Grisafi F., Brucato· A., 2016, Oscillation dynamics of free vortex surface in uncovered unbaffled stirred vessels, Chemical Engineering Journal, 285, 477-486

Hekmat D., Hebel D., Schmid H., Weuster-Botz D., 2007, Crystallization of lysozyme: from vapor diffusion experiments to batch crystallization in agitated ml-scale vessels. Proc. Bioch., 42, 1649–1654.

Micheletti M., Yianneskis M., 2004, Study of fluid velocity characteristics in stirred solid-liquid suspensions with a refractive index matching technique. Proceedings of the Institution of Mechanical Engineers, Part E: Jour. of Proc. Mech. Eng., 218 (4), 191-204.

Montante G., Paglianti A., 2014, Hydrodynamics of a model stirred anaerobic digester, Chem. Eng. Trans., 38, 49-54.

Oldshue, J. Y., 1983, Fluid Mixing Technology, McGraw-Hill, New York, NY.

Sardeshpande M.V., Kumar G., Aditya T., Ranade V.V., 2016, Mixing studies in unbaffled stirred tank reactor using electrical resistance tomography, Flow Measurement and Instrumentation, 47, 110-121.

Scargiali F., Busciglio A., Grisafi F., Tamburini A, Micale G., Brucato, A., 2013, Power consumption in uncovered unbaffled stirred tanks: Influence of the viscosity and flow regime. Ind. Eng. Chem. Res., 52, 14998-15005.

Scargiali F., Busciglio A., Grisafi F., Brucato A., 2014, Mass transfer and hydrodynamic characteristics of unbaffled stirred bio-reactors: influence of impeller design, Biochemical Engineering Journal, 82, 41- 47

Tamburini A., Gentile L., Cipollina A., Micale G., Brucato A., 2009, Experimental investigation of dilute solid-liquid suspension in an unbaffled stirred vessel by a novel pulsed laser based image analysis technique. Chem. Eng. Trans.,17 , 531-536. DOI: 10.3303/CET0917089.

Tamburini A., Cipollina A., Micale G., Brucato A., Ciofalo M., 2011a, CFD simulations of dense solid-liquid suspensions in baffled stirred tanks: Prediction of suspension curves, Chemical Engineering Journal, 178, 324-341

Tamburini A., Cipollina A., Micale G., Brucato A., 2011b, Dense solid-liquid suspensions in top-covered unbaffled stirred vessels. Chem. Eng. Trans., 24 , 1441-1446. DOI: 10.3303/CET1124241.

Tamburini A., Cipollina A., Micale G., Brucato A., 2012, Measurements of Njs and power requirements in unbaffled bioslurry reactors. Chem. Eng. Trans., 27, 343-348. DOI: 10.3303/CET1227058.

Tamburini A., Cipollina A., Micale G., Brucato A., Ciofalo, 2013a, CFD simulations of dense solid-liquid suspensions in baffled stirred tanks: Prediction of solid particle distribution, Chem. Eng. J., 223, 875-890.

Tamburini A., Cipollina, A., Micale G., Brucato, A., 2013b, Particle distribution in dilute solid liquid unbaffled tanks via a novel laser sheet and image analysis based technique. Chem. Eng. Sci., 87, 341-358.

Tamburini A., Brucato A., Busciglio A., Cipollina A., Grisafi F., Micale G., Scargiali F., Vella, G., 2014, Solid−Liquid suspensions in top-covered unbaffled vessels: influence of particle size, liquid viscosity, impeller size, and clearance. Ind. Eng. Chem. Res., 53, 9587-9599.

Tamburini A., Cipollina A., Micale G., Scargiali F., Brucato A., 2016, Particle Suspension in Vortexing Unbaffled Stirred Tanks, Ind. Eng. Chem. Res, 55 (27), 7535-7547.

Unadkat H., Rielly C.D., Hargrave G.K., Nagy Z.K., 2009, Application of fluorescent PIV and digital image analysis to measure turbulence properties of solid-liquid stirred suspensions. Chem. Eng. Res. Des., 87, 573-586.

Wang S., Parthasarathy R., Wu J., Slatter P., 2014, Optimum solids concentration in an agitated vessel, Industrial and Engineering Chemistry Research 53 (10), 3959-3973.